

# Synthesis and characterization of pure and doped ZnO nanoparticles

S. B. RANA, P. SINGH<sup>a</sup>, A. K. SHARMA<sup>b</sup>, A. W. CARBONARI<sup>c</sup>, R. DOGRA<sup>d\*</sup>

*Department of Electronics, Guru Nanak Dev University, Regional Campus - Gurdaspur, India.*

<sup>a</sup>*Department of Chemistry, Guru Nanak Dev University, Amritsar, India.*

<sup>b</sup>*Beant College of Engineering & Technology, Gurdaspur, India.*

<sup>c</sup>*Instituto de Pesquisas Energéticas e Nucleares, IPEN-CNEN, São Paulo, SP, Brazil.*

<sup>d</sup>*Beant College of Engineering & Technology, Gurdaspur-143521, India.*

In this work, a direct precipitation method using wet chemical reaction was used to synthesize pure and doped ZnO nanoparticles. The zinc nitrate and sodium hydroxide were used as starting materials to precipitate the desired nanoparticles followed by calcinations at temperatures of 500-700 °C. The phase purity and crystallite size of as grown particles were characterized via X-ray diffraction and scanning electron microscopy. The X-ray diffraction results indicated that the synthesized ZnO powders had a pure single phase wurtzite structure and the average particle sizes were about 40 nm. The dopant elements Co and Cu influenced the particle size of the powders. The formation of single phase ZnO powders was also confirmed by nuclear hyperfine method such as perturbed angular correlation spectroscopy which revealed the incorporation of dopants at the substitutional zinc sites in ZnO lattice.

(Received January 10, 2009; accepted February 18, 2010)

*Keywords:* ZnO, Nanoparticle, Co, Cu dopants, XRD

## 1. Introduction

There is growing interest in II-VI compound semiconductor ZnO because of its direct band-gap of 3.37 eV at room temperature with a large exciton binding energy of 60 meV which have optoelectronic applications in the blue, violet and ultra-violet regions of the electromagnetic spectrum [1]. Recently, semiconductor nanoparticles of ZnO have also received much recognition as a potential candidate material for solar energy conversion, varistors, luminescence, electrostatic dissipative coatings, transparent UV protection films, chemical sensors, spintronic devices etc. [2-7], due to their unusual electrical, optical, mechanical and magnetic properties, which results from quantum confinement effects. In order to better understand these properties of pure and doped nanoparticles of ZnO, the choice of sample preparation method therefore is of greatest importance. The preparation method should be the one that can compel the doped ions into substitutional site and have atomic scale homogeneous mixing with host atoms without the formation of secondary phases, nanoclusters etc. For the same, extensive research efforts have been carried out worldwide to synthesize nano-sized particles using various methods [8-14] such as thermal decomposition, chemical vapor deposition, sol-gel, spray pyrolysis, microemulsions and precipitation. Among these synthesis methods, precipitation method compared with other traditional methods provides a simple growth process for large-scale production, and which of course is an efficient and inexpensive way. The distinctive feature of this process is

that an atomic scale homogeneous distribution of doped ions in the host matrix can be achieved.

The aim of the present study is to synthesize phase pure nanoparticles of pure and doped ZnO via direct precipitation method followed by structural characterization using X-ray diffraction (XRD), energy dispersive x-ray spectroscopy (EDS), scanning electron microscopy (SEM) and atomic scale characterization for homogeneous distribution of dopants in the host matrix of ZnO using nuclear hyperfine method such as perturbed angular correlation (PAC) spectroscopy, the details of which are given in the most recent review article [15]. The PAC technique is based upon the hyperfine interaction of the nuclear electric quadrupole moment or magnetic moment of the probes, respectively, with the electric field gradient (EFG) or magnetic hyperfine field arising from the extra-nuclear electronic charges and spin distributions respectively. Thus, PAC spectroscopy requires the introduction of radioactive probe into the crystal lattice that decays to the excited level of a daughter isotope and populates an isomeric state of interest through a  $\gamma$ - $\gamma$  cascade. Since this technique offers a high degree of sensitivity to local structural variations in the crystal lattice, the PAC can be used to follow changes such as bond distances, local symmetry, defect trapping/detrapping, magnetic spin distributions, etc. on microscopic scale and, thereby, images the chemical environment around the probe atoms.

## 2. Experimental details

A direct precipitation method, which is briefly summarized in Figure 1, was used to synthesize the nanoparticles of pure and doped ZnO. Zinc nitrate ( $\text{Zn}(\text{NO}_3)_2$ ) and sodium hydroxide ( $\text{NaOH}$ ) were used as precursors of the ZnO particles. The aqueous solution of metal nitrates was prepared from pure metal (99.999%) by dissolving in concentrated nitric acid. A known quantity of  $\text{NaOH}$  was dissolved in deionised water and the resulting solution was mixed with the zinc nitrate solution leading to the formation of white precipitates. The precipitates were washed several times with deionised water and finally with ethyl alcohol to remove the impurities. The resulting fine powder was dried in an oven at  $100^\circ\text{C}$  for 15h. The as dried powder was grounded and then calcined at different temperatures ( $500$  and  $700^\circ\text{C}$ ) for 4h. For present study, we prepared pure ZnO, and doped  $\text{Zn}_{1-x}\text{T}_x\text{O}$  ( $\text{T}=\text{Co}$  and  $\text{Cu}$ ) for which the stoichiometric amount of respective metal nitrate was dissolved in the zinc nitrate solution before precipitation. Phase purity of the powder samples was examined by (XRD) using  $\text{Cu K}_\alpha$  radiation,  $40\text{kV}$  and  $30\text{mA}$ , time constant of  $0.5\text{s}$  and crystal graphite monochromator. With increasing annealing temperature, the typical tendency of increasing intensity of all the peaks in XRD pattern was observed. From XRD line broadening, the average particle sizes for nanocrystalline powders were deduced using Scherrer's equation ( $D = 0.9\lambda / \beta \cos \theta$ , where  $D$  is the crystallite diameter,  $\lambda$  is the radiation wavelength and  $\theta$  the incidence angle).

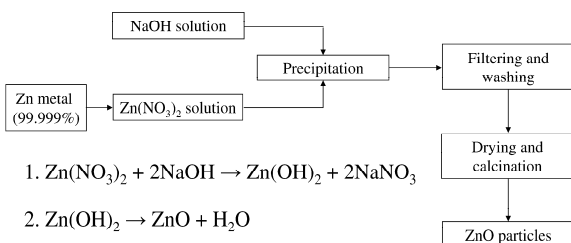


Fig. 1. Schematic of sample preparation using precipitation method. The chemical reactions involved for the formation of ZnO particles are also given.

The value of  $\beta$  was determined from the experimental integral peak width. Values were corrected for instrumental broadening. The composition studies were done by energy dispersive x-ray spectroscopy. The particle size and morphology of the calcined particles was observed using scanning electron microscopy. In order to carry out the PAC measurements, approximately  $10\ \mu\text{Ci}$  of  $^{111}\text{InCl}_3$  solution was added to the metal nitrate solution before precipitation. The PAC measurements were performed on these powders using four conical  $\text{BaF}_2$  scintillator based spectrometer [15] at room temperature. The present data were analyzed by considering a simple model consisting of two fractions of probe atoms: (a) fraction  $f_1$  corresponding to the probe atoms sitting on

regular lattice sites experiencing a unique EFGs and (b) fraction  $f_2$  corresponding to the probe atoms in a heavily disturbed environment, i.e., experiencing strong and non-unique EFGs giving rise to large EFG distribution.

## 3. Results and discussions

Fig. 2 reports the typical XRD spectra of pure and doped ZnO powders. In order to compare the sample preparation method, an XRD pattern of a commercial ZnO powder is also shown in Figure 2. Three pronounced ZnO diffraction peaks (100), (002) and (101) appear at  $2\theta = 31.72^\circ$ ,  $34.38^\circ$  and  $36.22^\circ$ , respectively. The crystallite size of ZnO particles which was deduced from Scherrer's equation, gave the values of about  $34\ \text{nm}$  and  $40\ \text{nm}$  for ZnO powders, respectively, annealed at  $500^\circ\text{C}$  and  $700^\circ\text{C}$ . The XRD data were refined by the Rietveld method using the program Rietica and the extracted lattice constants are given in Table 1. Both pure and doped ZnO powders presented wurtzite type crystal structure (hexagonal) with  $\text{P6}_3\text{mc}$  space group [16]. The lattice constants calculated from the XRD pattern for pure ZnO annealed at  $700^\circ\text{C}$  are  $a = 3.2475\ \text{\AA}$  and  $c = 5.2013\ \text{\AA}$  and are close to the lattice constants  $a=3.2488\ \text{\AA}$  and  $c=5.2061\ \text{\AA}$  given in the standard data (JCPDS, 36-1451). Diffraction peaks related to the impurities were not observed in the XRD pattern, confirming the high purity of the synthesized powder.

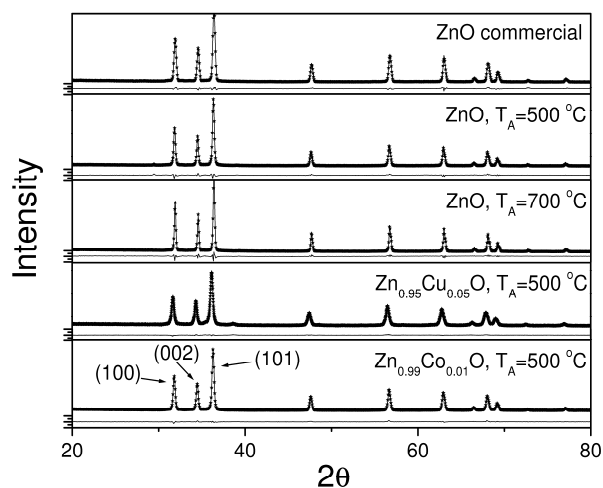


Fig. 2. The observed X-ray powder-diffraction spectra for pure and doped ZnO. The solid lines represent the calculated pattern with the Rietveld method. The residuals are shown in the lower part of each spectrum.  $T_A$  represents annealing temperature.

The lattice constants did not show any significant shift for Co-doped ZnO powders which is because of the fact that the ionic radii in the case of zinc and cobalt dopants are quite similar (i.e.  $\text{Zn}^{2+}=0.60\ \text{\AA}$ ,  $\text{Co}^{2+}=0.58\ \text{\AA}$ ). On the other hand for Cu-doped ZnO, both the lattice constants increased slightly with the incorporation of Cu which is

consistent with the fact that the radius of  $\text{Cu}^{2+}$  (0.73 Å) is larger than that of  $\text{Zn}^{2+}$  (0.60 Å) in their tetrahedral coordinations. The reduction of particle size (as given in Table 1) was also observed from XRD pattern for doped ZnO powders with the incorporation of Co and Cu dopants in the ZnO lattice. This may be explained by the reduction of sintering rate due to incorporation of dopant atoms into the ZnO lattice.

Table 1. The lattice constants as obtained from Rietveld refinement and particle size as deduced from X-ray line broadening.

Sample	$a$ (Å)	$c$ (Å)	Particle size (nm)
Commercial ZnO	3.2475	5.2023	28
ZnO annealed at 500 °C	3.2467	5.2007	34
ZnO annealed at 700 °C	3.2475	5.2013	40
$\text{Zn}_{0.99}\text{Co}_{0.01}\text{O}$ annealed at 500 °C	3.2474	5.2012	29
$\text{Zn}_{0.95}\text{Cu}_{0.05}\text{O}$ annealed at 500 °C	3.2663	5.2313	24

Fig. 3 shows the SEM images of ZnO powders synthesized at 500 °C and 700 °C. The powders calcined at 500 °C were homogeneous and agglomerated with a grain size of 80 nm. The increasing calcination temperature leads to the trend of increasing grain size which is believed to be affected by the promotion of crystalline phase in the powder and neck growth between particles as temperature increased. The grain size of crystallites in ZnO powders calcined at 700 °C was observed to be more than 100 nm. The grain sizes as measured by XRD and SEM were quite different. In SEM, the grain size was measured by the difference between the visible grain boundaries whereas in XRD, the measurement was extended to the crystalline region that diffracted X-rays coherently. Therefore, the XRD measurements led to smaller size. The SEM images of doped samples indicate that the samples were homogeneous with dopants (Co or Cu) substituting Zn sites in ZnO compound and do not contain any other dopant dominating phases. The EDS results as shown in Figure 4 indicate that no other element but Zn and O were present in pure ZnO samples whereas Zn, dopants and O were present in doped samples. The small Pt peak appearing in the spectra is due to the coating of the sample surface required for the measurements.

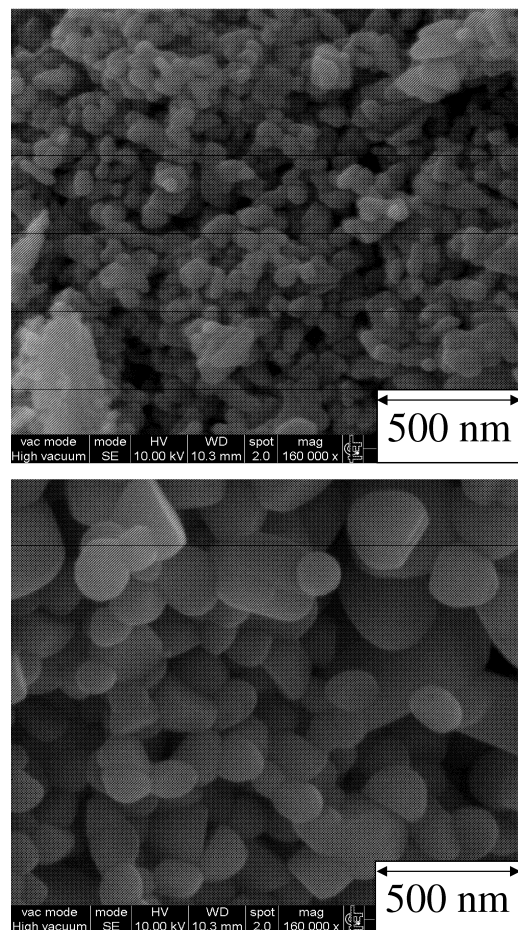


Fig. 3. SEM images of pure ZnO nano-sized particles. Top: ZnO,  $T_A=500$  °C; Bottom: ZnO,  $T_A=700$  °C.  $T_A$  represents annealing temperature.

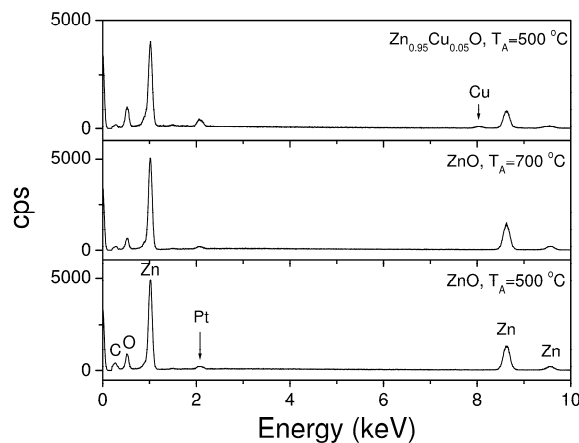


Fig. 4. EDS spectra for pure and Cu-doped ZnO particles.  $T_A$  represents annealing temperature.

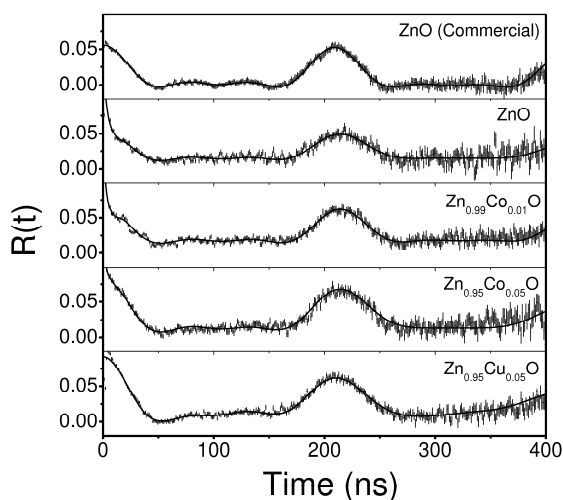


Fig. 5. Room temperature PAC spectra for pure and doped ZnO powders with  $^{111}\text{In}/^{111}\text{Cd}$  radioisotope probe atoms. The solid lines represent least-squares fit to the PAC spectra with the appropriate theoretical function as given in references [15, 20].

The formation of single phase ZnO having wurtzite structure in the synthesized ZnO powders was further supported by PAC measurements. The least-squares fitted PAC spectra measured with  $^{111}\text{In}$  probes for the pure and doped ZnO nanopowders are shown in Figure 5, PAC spectrum for commercial sample of ZnO was also acquired at room temperature. The environment of the  $^{111}\text{In}$  probe atoms in the ZnO nanoparticles is characterized by two sites corresponding to probe atoms sitting at substitutional sites in ZnO lattice leading to unique value of EFG ( $1.51 \times 10^{21} \text{ V/m}^2$  corresponding to quadrupole interaction frequency of 30.6 MHz) and to probe atoms at the surface of the nanoparticles leading to highly disordered non-unique EFG with large distribution. Least-squares fit to the data yields that most of the probe atoms are incorporated in highly disordered, non-unique lattice environments which is quite obvious for nano-sized particles when probe atoms are residing on the surface of the nanocrystalline particles, having large surface to volume ratio. For all the samples, the measured EFG remained same within errors. The measured EFGs in pure and doped ZnO nanopowder for  $^{111}\text{In}$  probe are consistent with the results of earlier PAC measurements in nano-crystalline, bulk ZnO [17-19] and single crystal of ZnO [20]. As the hexagonal Wurtzite and the zinc blende lattices are quite similar in terms of their nearest neighbors; one must expect small EFGs at the cation/anion sites in both lattices. Therefore, the observed small EFG was attributed to the substitutional incorporation of the probe atoms at the cation-sites in the distorted oxygen tetrahedron [20]. The PAC measurements did not reveal the presence of any contaminated phases related to the dopants which equivalently indicate that the dopants are homogeneously distributed in the ZnO lattice.

#### 4. Conclusions

Nano-sized ZnO particles were successfully synthesized via direct precipitation route using wet chemical reaction method. XRD and SEM analysis confirmed the formation of single phase nanoparticles of pure and doped ZnO. The Rietveld analysis of XRD pattern showed only the presence of pure wurtzite crystal structure in all the samples with an average particle size of about 40nm, which may find their applications as UV shielding material. The elemental analysis of the synthesized nanoparticles measured by EDS showed no other element but Zn and O are present in pure ZnO, and Zn, only dopants and O are present in doped samples. The PAC measurements reveal that Co and Cu are incorporated at zinc sites and do not change the wurtzite structure of ZnO lattice. The current synthesis method using chemical reaction will be extended to prepare nanocrystalline powders of Sb- and As- doped ZnO which are thought to be potential candidate for p-type conduction.

#### References

- [1] Ü. Özgür, Ya. I. Alivov, C. Liu, A. Teke, M. A. Reshchikov, S. Doğan, V. Avrutin, S. -J. Cho, H. Morkoç; *J. Appl. Phys.* **98**, 041301 (2005).
- [2] S. N. Bai, T. Y. Tseng, *J. Appl. Phys.* **74**, 695 (1993).
- [3] M. Aslam, V. A. Chaudhary, I. S. Mulla, S. R. Sainkar, A.B. Mandale, A.A. Belhekar, K. Vijayamohan, *Sens. Actuators A-phys.* **75**, 162 (1999).
- [4] O. Kluth, B. Rech, L. Houben, S. Wieder, G. Schope, C. Beneking, H. Wagner, A. Löffl, H.W. Schock, *Thin Solid Films* **351**, 247 (1999).
- [5] N. K. Zayer, R. Greef, K. Roger, A. J. C. Grellier, C. N. Pannell, *Thin Solid Film* **352**, 179 (1999).
- [6] S. J. Pearton, C. R. Abernathy, D. P. Norton, A. F. Hebard, Y. D. Park, L. A. Boatner, J. D. Budai, *Mater. Sci. Eng. R* **40**, 137 (2003).
- [7] F. Pan, C. Song, X. J. Liu, Y. C. Yang, F. Zeng, *Mater. Sci. Eng.* **R62**, 1 (2008).
- [8] S. M. Haile, D. W. Johnson, G. H. Wiseman, H. K. Bowen, *J. Am. Ceram. Soc.* **72**, 2004 (1989).
- [9] M. Andres-Verges, M. Martinéz-Gallego, *J. Mater. Sci.* **27**, 3756 (1992).
- [10] C. H. Lu, C.H. Yeh, *Ceram. Int.* **26**, 351 (2000).
- [11] X. Y. Kang, T. D. Wang, Y. Han, M. D. Tao, *Mater. Res. Bull.* **32**, 1165 (1997),.
- [12] C. H. Lu, C. H. Yeh, *Mater. Lett.* **33**, 129 (1997).
- [13] X. Y. Zhao, B. C. Zheng, C. Z. Li, H. C. Gu, *Powder Technol.* **100**, 20 (1998).
- [14] J. Wang, L. Gao, *Inor. Chem. Com.* **6**, 877 (2003).
- [15] R. Dogra, A.P. Byrne, M.C. Ridgway, *J. of Electronic Material* **38**, 623 (2009).
- [16] D. A. A. Santos, A. D. P. Rocha, M. A. Macêdo, *Powder Diff Suppl* **23**, S36 (2008).

- [17] Th. Agne, Z. Guan, X. M. Li, H. Wolf, Th. Wichert, H. Natter, R. Hempelmann, *Appl. Phys. Lett.* **83**, 1204 (2003).
- [18] S. Deubler, J. Meier, R. Schütz, W. Witthuhn, *Nucl. Instrum. Meth. B* **63**, 223 (1992).
- [19] W. Sato, Y. Itsuki, S. Morimoto, H. Susuki, S. Nasu, A. Shinohara, Y. Ohkubo, *Phys. Rev. B* **78**, 045319 (2008).
- [20] R. Dogra, A. P. Byrne, M. C. Ridgway, *Optical Materials* **31**, 1443 (2009).

---

\*Corresponding author: drdogra@yahoo.com